



## Research Article

# Sulfate and chloride resistance of bottom ash doped slag-based geopolymer composites

Yurdakul AYGÖRMEZ<sup>1,\*</sup>

<sup>1</sup>Department of Civil Engineering, Yildiz Technical University, Istanbul, Türkiye

## ARTICLE INFO

### Article history

Received: 16 April 2021

Revised: 16 July 2021

Accepted: 28 September 2021

### Keywords:

Geopolymer; Slag; Bottom Ash; Magnesium Sulfate; Sodium Sulfate; Sodium Chloride

## ABSTRACT

Within the scope of this study, while the performance of slag (S)-based geopolymer mortars with bottom ash (BA) reinforcement was examined, chloride and sulfate attack tests were also carried out to investigate their durability properties. For the durability tests of geopolymer composites, sodium chloride (NaCl) and sodium and magnesium sulfate ( $\text{Na}_2\text{SO}_4$  and  $\text{MgSO}_4$ ) solutions were preferred for a period of 10 months and a 15% solution percentage. The performance of geopolymer composites after the effect of durability was determined by flexural and compressive strengths, SEM and XRD analyses, weight changes, and visual inspection. When the results obtained were evaluated, it was seen that 15% BA substitution provided the highest compressive strength. There was variation in durability tests. At the end of the 2-month period, there was an increase in the compressive strength, while a decrease was observed at the end of the 6-month period. The main factor that created these fluctuations was that alkali ions migrated from sample to solution while the solutions were diffusing into the matrix. Gypsum and ettringite formed in the pores were effective in the losses that occurred in the 6-month period. In addition, the alkali ions leaving the sample and passing into the solution effectively accelerated the formation of micro cracks. Thus, strength losses were observed.

**Cite this article as:** Aygörmez Y. Sulfate and chloride resistance of bottom ash doped slag-based geopolymer composites. Sigma J Eng Nat Sci 2023;41(2):288–301.

## INTRODUCTION

Geopolymer creates an alternative product by causing lower carbon emissions, unlike Portland cement-based binders. Geopolymer products are produced using precursor materials containing amorphous aluminosilicate in their structure. In addition, an alkali activator (chemical liquid solution providing high pH) consisting of a

mixture of silicate and hydroxide is used in geopolymerization. While a ceramic-like amorphous microstructure is formed by the reaction between the binder material and the activator, this reaction also includes melting and condensation [1].

As the information about the solutions it brings to carbon dioxide emission has expanded, the search for replacing alternative binders with cement has accelerated. Bakis

### \*Corresponding author.

\*E-mail address: [aygormez@yildiz.edu.tr](mailto:aygormez@yildiz.edu.tr)

This paper was recommended for publication in revised form by Regional Editor Metin Tülü



et al. [2] produced 8 different series by replacing normal strength control concrete with pumice. By using fiber and city water, 86.55 MPa of compressive strength and 11.12 MPa of flexural strength were obtained. Bayraktar et al. [3] investigated the stabilization of electric arc furnace powders obtained during steel production from scrap metals with different ratios of cement and low-grade MgO. It has been determined that the environmental performance or structural properties were suitable if the electric arc furnace powders were used at a percentage of 30% by weight. Uslu et al. [4] did not encounter any significant problems when the chemical treatment sludge produced in the automotive factory was used up to 10% as a raw material component in brick manufacturing. In addition to the use of substitute materials in this way instead of cement, the production of geopolymer has also created an environmentally important alternative.

Slag is a waste product from the pig iron production process, which consists mainly of calcium-magnesium aluminosilicate glass. The structure, properties, and chemical composition vary depending on the raw materials and industrial process. The most commonly used slag is blast furnace slag. As a result of the main reactions for alkali-activated slag, high strength results were obtained due to the calcium silicate hydrate (C-S-H) product. However, despite high strength, drying shrinkage values were high due to insufficient workability and rapid setting [5-6]. Bottom ash is a granular, dark gray, and porous material obtained during the coal burning process. Since the bottom ash has an aluminum oxide-silicate structure, geopolymerization can be performed between alkaline solution and aluminosilicate with alkali activation [7]. It has been tried in the production of geopolymer, especially after it has been made fine-grained. Higher-strength values were obtained under room conditions and heat curing [8-9]. However, durability studies are limited, especially in the case of bottom ash use. More research needs to be done on this subject.

Sulfate attack is one of the vitally important durability indexes for concrete and mortar materials. In studies of sulfate attack on conventional Portland Cement concrete, the reaction between sulfate-containing solutions and hydration products has a complex mechanism [10-11]. Bakharev et al. [12] determined that the performance of geopolymers against sulfate attack was different. The main parameters affecting the stability of geopolymer composites are the cation and concentration in the sulfate environment and the alkali activator type. It has been observed that geopolymer mixtures prepared using only sodium hydroxide were more stable against sulfate attack than the samples prepared together with sodium silicate and hydroxide or prepared by using potassium silicate and hydroxide together. When the performance research of geopolymers exposed to 5% magnesium sulfate and 5% sodium sulfate solutions in different combinations was carried out, it was seen that the changes in the composite

samples were small and the fluctuations in the mechanical properties were highest in the series in which the two solutions were used together. Fernández-Jiménez et al. [13] investigated the resistance of fly ash-based alkali-activated samples to the effect of sulfate. After fluctuation in the first stages, an increase in strength was detected both in air-cured samples and in samples kept in 4.4% Na<sub>2</sub>SO<sub>4</sub> solutions. After being kept in Na<sub>2</sub>SO<sub>4</sub> solution for 365 days, it was observed that the crystals of Na<sub>2</sub>SO<sub>4</sub> salts formed in the pores, and some deterioration occurred in this situation. Despite this situation, it has been observed that alkalinized materials perform satisfactorily. High solution concentrations have not been studied much, although the real environment tends to be more complex and extreme and this poses greater challenges for concrete and mortar structures.

A large number of performance studies have been conducted against the effects of chloride and sulfate on geopolymer composites and Portland Cement-based samples. Although there are many studies on the performance of geopolymer composites against these effects, studies on the reinforcement of slag-based geopolymers with bottom ash are limited. In this study, the performance of slag-based geopolymer samples containing up to 30% bottom ash was investigated, while their behavior under the influence of chloride and sulfate with a concentration of 15%, as opposed to solution attacks with low concentrations, was also investigated. Thus, it enables researchers in the construction industry to make promising designs for various applications. Three different periods were used to test the geopolymer samples. 2, 6, and 10-month solution attacks were made. After the completion of each solution period, the changes in flexural strength, compressive strength, and weight were investigated. In addition, SEM and XRD analyzes were conducted for examining the magnesium sulfate effect, and a visual inspection was performed after the magnesium sulfate test.

## MATERIALS AND METHODS

### Materials

The main binder material was used as slag for this study. The specific gravity value of the slag is 2.91 and the total silica + alumina + iron oxide ratio is 54.8%. The important feature of the slag is its calcium content and accordingly, it shortens the setting time. Bottom ash was used as the other binding material. In order to increase the reactivity of the bottom ash, it was ground to a 5% residue on a 45 µm sieve. The specific gravity of the bottom ash is 2.3. It was made into smaller particles to have a high specific surface. Due to this situation, it has become more reactive. The Blaine fineness values of bottom ash and slag are 5300 cm<sup>2</sup>/g and 4500 cm<sup>2</sup>/g, respectively. The chemical composition of the binders used is shown in Table 1.

**Table 1.** Binder materials' chemical analysis

Chemical analysis, %	SiO <sub>2</sub>	Fe <sub>2</sub> O <sub>3</sub>	Al <sub>2</sub> O <sub>3</sub>	MgO	CaO	Na <sub>2</sub> O	K <sub>2</sub> O	L.O.I.
Slag	40.60	1.37	12.83	6.87	36.08	0.79	0.68	0.78
Bottom ash	54.88	14.52	19.17	3.06	6.72	0.41	0.08	1.16

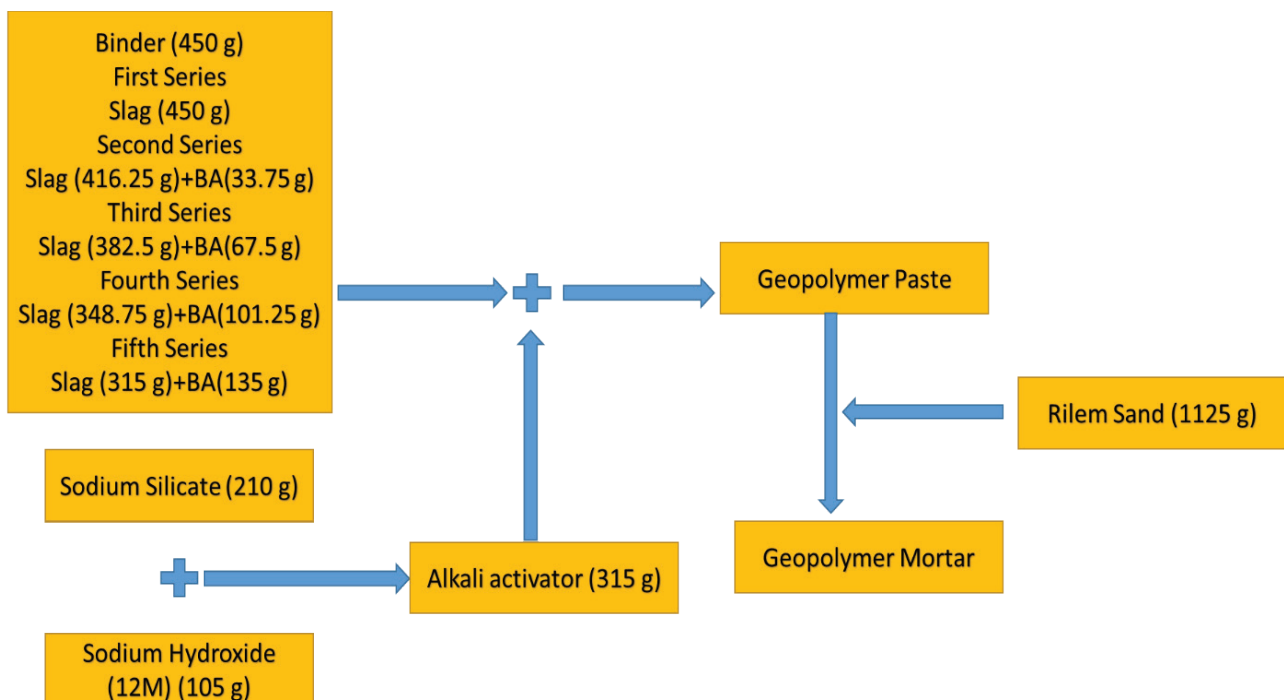
Rilem sand was used as the aggregate, and the unit weight and specific gravity values are 1.35 kg/m<sup>3</sup> and 2.6, respectively. Rilem sand has a water absorption rate of 1.276% and its properties comply with BS EN 196-1. A mixture of sodium silicate and hydroxide was used to prepare the activator. The SiO<sub>2</sub>/Na<sub>2</sub>O ratio was 3.29 in sodium silicate and the hydroxide was prepared as 12M.

### Specimen Mix Design

Within the scope of the geopolymer mortar study, slag and bottom ash were used as binding materials, standard sand as aggregate, and sodium silicate and hydroxide as activators. The sodium silicate/sodium hydroxide ratio was kept as 2:1, the aggregate/binder material was 2.5:1, and the binder material/activator ratio was 1:0.7, while water was evaluated only for preparing sodium hydroxide solution. Extra water wasn't added and a superplasticizer was added to keep the binder/activator ratio constant. For this reason, the activator/binder ratio was used instead of the water/binder ratio in the traditional Portland Cement based mortar. In total, 5 series were prepared and the mixture amounts for standard 450 g were summarized in Figure 1.

In addition, a detailed mixture description was made for the mortar sample containing 100% slag, and the difference in the other series was in the amount of bottom ash.

For the control mixture containing 100% slag, sodium hydroxide solution was prepared as 12M the day before. The hydroxide solution cooled at room temperature was first mixed with sodium silicate solution on the day of mixing. Here, the sodium silicate/sodium hydroxide ratio was taken as 2:1 and the activator was prepared. Then, a mixer drill was used for mixing the activator with 450 g of slag. The activator/binder material ratio was taken as 0.7:1. At the last stage, Rilem sand was added to the mixture at a ratio of 2.5:1 aggregate/binder, and the mixture was continued until a homogeneous mixture was obtained with a mixer drill. Two types of molds, 40 x 40 x 160 mm prism and 50 mm cube molds, were used. The homogeneous mixture was placed in the molds in two stages and vibration was applied at each stage. After the vibration was applied, the specimens were hardened in the mold for 2 hours. The samples were taken out of the mold at the end of this period with the early setting property of slag. After demolding, the specimens were retained at room temperature and relative

**Figure 1.** Mixture description for samples (g).

humidity (50±4%) for 28 days. Then, durability tests were started. The details are given in Table 2. Along with the control series, the other four series were prepared using bottom ash (7.5%, 15%, 22.5%, and 30%).

**Table 2.** The 5 series' details.

Mix ID	Binder material percentage
S	100% S
7.5BA	92.5% S+ 7.5% BA
15BA	85% S+ 15% BA
22.5BA	77.5% S+ 22.5% BA
30BA	70% S+ 30% BA

### Test Procedure

Three different 15% solutions (sodium chloride and sulfate, and magnesium sulfate) were prepared for durability tests and poured into plastic storage boxes. The prepared samples were first kept in an oven for one day at 105°C. The main reason for this was to increase the efficiency of the solution by increasing its absorption. Solution concentration and pH values must be maintained to create a homogeneous structure in the test. Therefore, the solutions were renewed at the end of the 1<sup>st</sup>, 2<sup>nd</sup>, and 6<sup>th</sup> months. 4 units of solution for 1 unit of the sample were placed in the plastic box. The samples were taken out of the plastic boxes after 2 months, 6 months, and 10 months and left to dry by keeping at room temperature. A wire brush was used for cleaning the outer surface after the specimens dried. The flexural strength, compressive strength, and weight changes at the end of three different periods were compared with the 28-day conditions. The compressive strength was found using cube specimens (50 mm) and the flexural strength was found using prism specimens (40x40x160 mm). Three samples were used for the tests and the final values were found according to the average. In addition, microstructural analyzes were also applied to the samples. After the magnesium sulfate test, a visual inspection was done. The SEM and XRD analyzes were conducted according to the magnesium sulfate test.

## RESULTS AND DISCUSSION

### Strength Results

The mechanical properties of the slag-based geopolymer composites produced by adding bottom ash and the results of the residual compressive strength after chloride and sulfate attacks are given together (Figures 2-4). When the details are examined, the interactions between the slag and the bottom ash are explained: Slag was an important geopolymer binder material due to its oxide components and mineralogical structure. It contained a significant amount of basic oxides such as CaO and MgO, which could

be dissolved at a higher rate by the geopolymerization process. Due to the hydration products obtained with MgO and CaO, the slag had a driving force in geopolymerization. Due to the slag, more CSH, CASH, and NASH formations were observed, while a more homogeneous and dense structure was formed by connecting the voids between the unreacted particles and different hydrated phases. In this way, slag-based geopolymer mortars could be cured at room conditions without the need for temperature curing. However, slag-based geopolymer mortars had disadvantages such as early hardening, rapid slump loss, and workability. Alternative binders should be investigated in this situation [14-18]. Bottom ash was used for this purpose. When the bottom ash, whose pozzolanic reaction was increased by bringing it to high fineness, was used up to 15%, it formed an increase in the strength results. Having a high percentage of silica and alumina was an important factor in this case. These components supported the formation of geopolymerization products (CSH, CASH, and NASH) that strengthened strength development by reacting with alkali silicate solutions. In addition, by increasing the free calcium ion (Ca<sup>2+</sup>) ratio in the composition, bottom ash supported the formation of calcium silicate hydrate (CSH) gel as a result of the reaction with the silicate. In addition, its high thinness also played a role in the development of strength by showing a filling effect. Using it at a higher ratio caused a decrease in strength. Its high thinness increased the specific surface area while increasing the need for activators. While the decrease in flowability and workability created a more hollow structure, it also caused a decrease in strength [15, 19-22].

Figures have been studied in detail. It was observed that the geopolymer composites gained strength after the solution effect period of 2 months was completed. This showed that the initial solution effect helped the geopolymerization to continue. Particularly, the calcium expansion products from the slag reacted with sulfate and chloride crystals to renew the pore structure, increasing the compactness of the geopolymer structure [23]. After 2 months, chloride and sulfate attacks increased, creating more porosity, and microcracks also increased. Thus, strength losses started to be seen due to erosion. If the magnesium sulfate solution was taken as a basis, the fluctuations in the strength results can be explained. There are two kinds of movements. The first of these movements was the transition of alkali ions to the solution by leaving the sample, and the second was the diffusion of Mg into the sample [12, 24]. At first, the second movement provided the continuation of the geopolymerization, but later it caused a loss of strength with deterioration. Waiting in the oven before the test allowed the samples to absorb the solutions better. The temperature increased the void ratio and increased the absorption tendency. After 2 months, the formation of gypsum and ettringite in the pores increased the microcracks, while the transition of alkalis to the solution increased the strength loss [12, 25]. When comparing the solutions, it was seen that the most

aggressive solution was magnesium sulfate. Due to this situation, the most mechanical losses were due to magnesium sulfate. The chloride ions' smaller size resulted in higher penetration. So, the highest strength increases were in sodium chloride solution [26-27].

After 2, 6, and 10 months, residual compressive strengths of 43.92 MPa, 28.51 MPa, and 19.06 MPa were obtained for the 15BA sample under the influence of magnesium sulfate. After 2, 6, and 10 months, residual compressive strengths of 47.83 MPa, 32.23 MPa, and 24.81 MPa were obtained

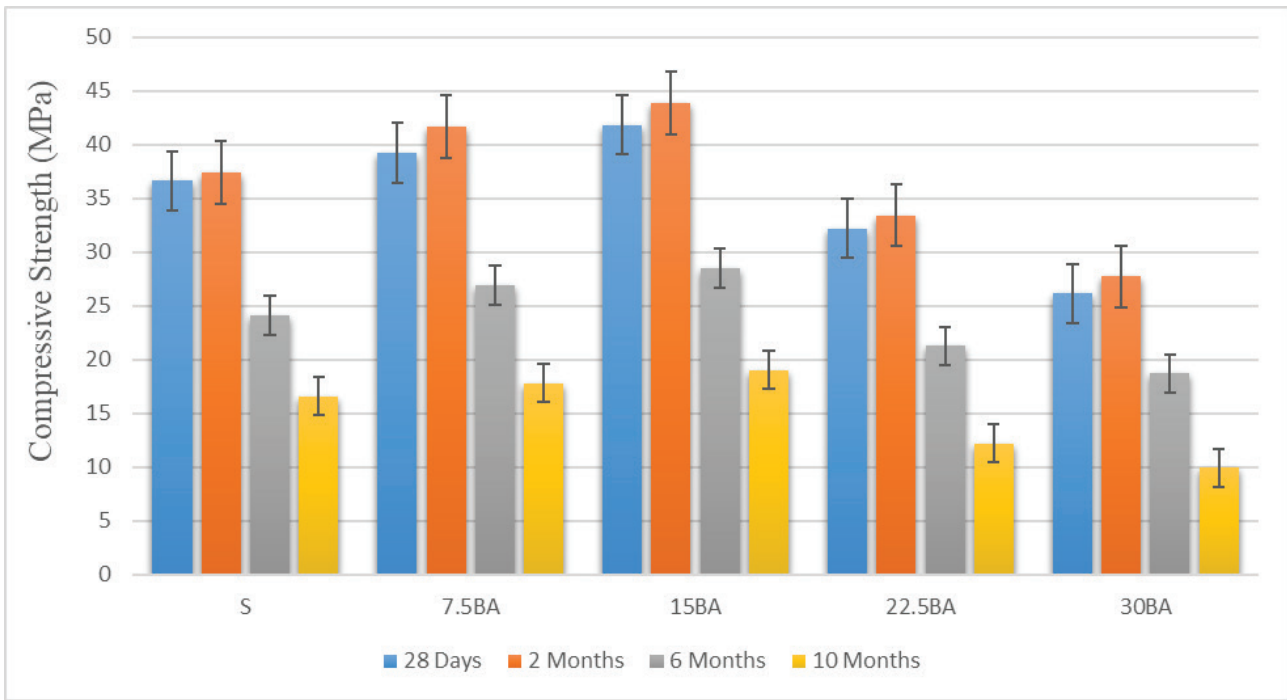


**Figure 2.** Compressive strength results with magnesium sulfate exposure.

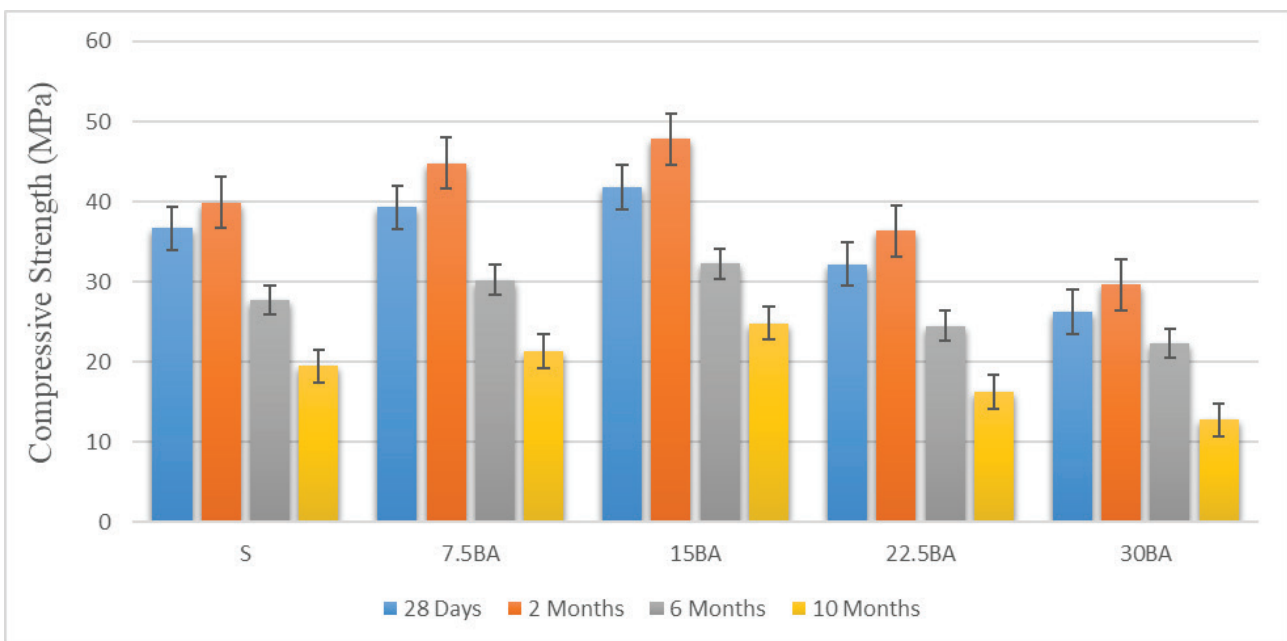


**Figure 3.** Compressive strength results with sodium sulfate exposure.

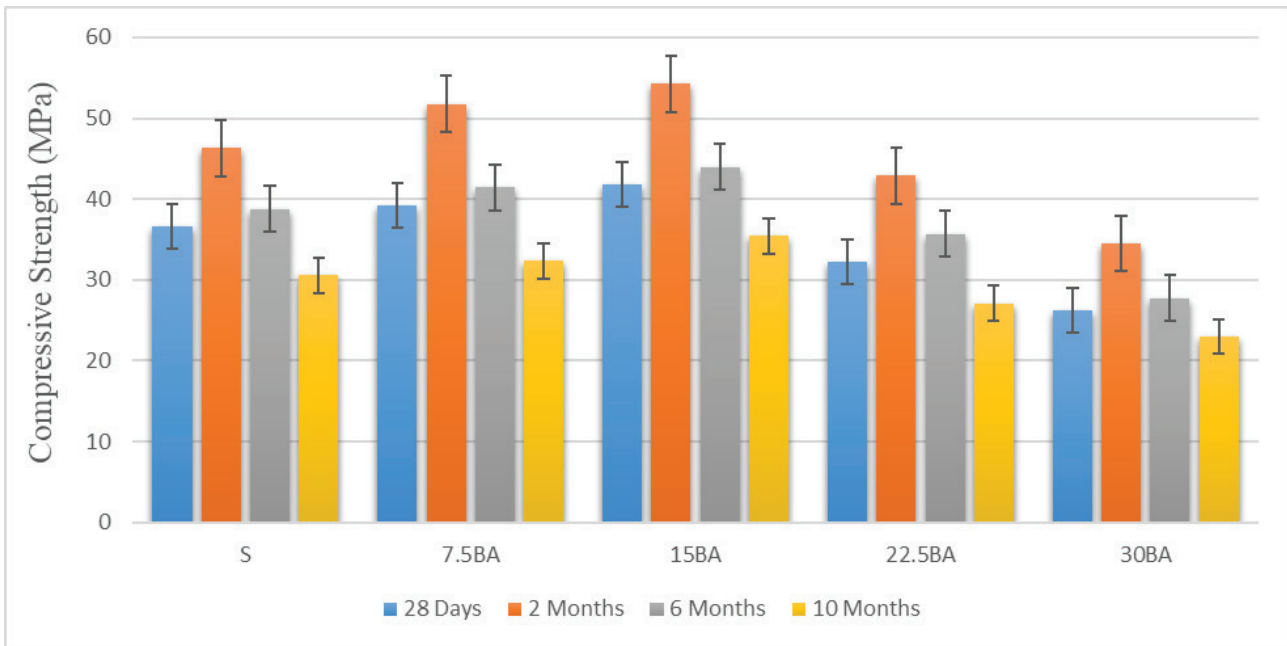


Figure 4. Compressive strength results with sodium chloride exposure.

for the 15BA sample under the influence of sodium sulfate. After 2, 6, and 10 months, residual compressive strengths of 54.23 MPa, 43.96 MPa, and 35.45 MPa were obtained for the 15BA sample under the influence of sodium chloride.

The 28-day flexural strengths of the bottom ash reinforced samples are given in comparison with the results after the effect of sulfate and chloride (Figures 5-7). The flexural strength results showed a decrease directly after solution

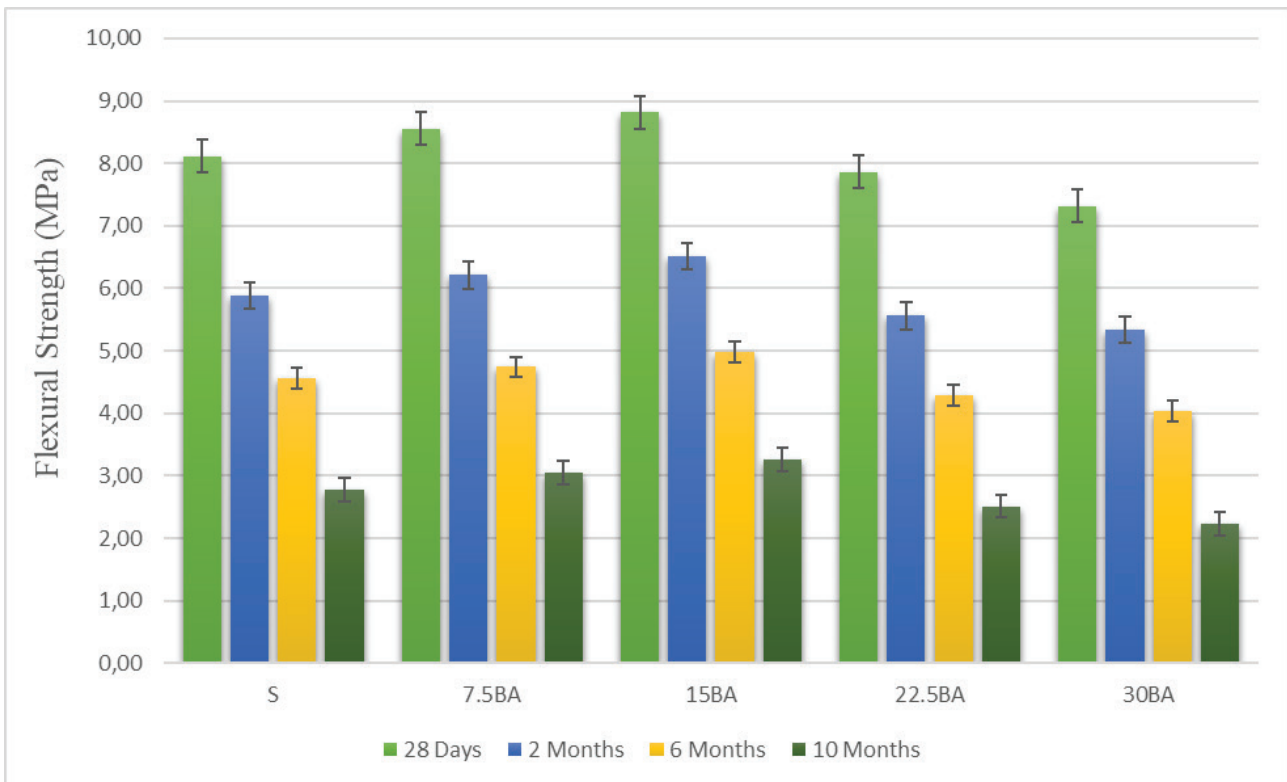


Figure 5. Flexural strength results with magnesium sulfate exposure.

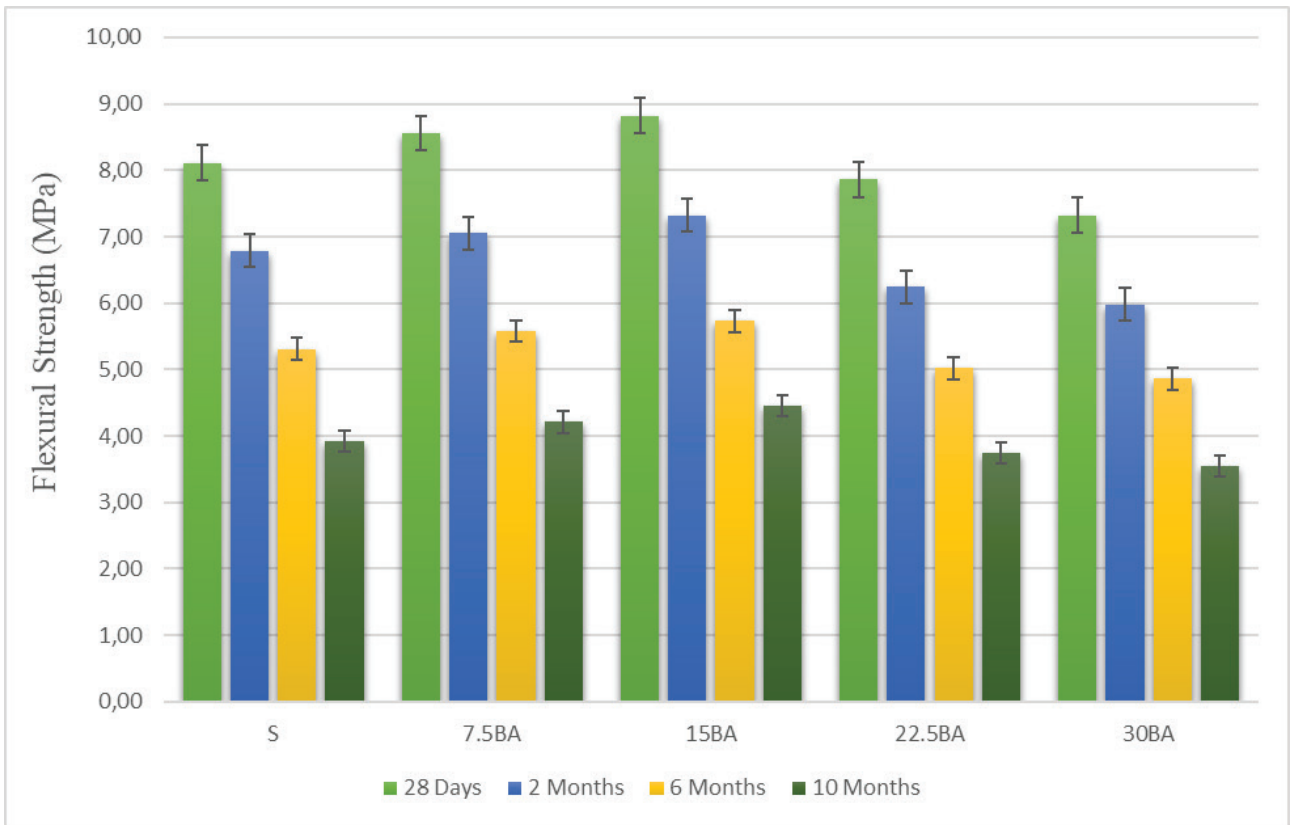


Figure 6. Flexural strength results with sodium sulfate exposure.

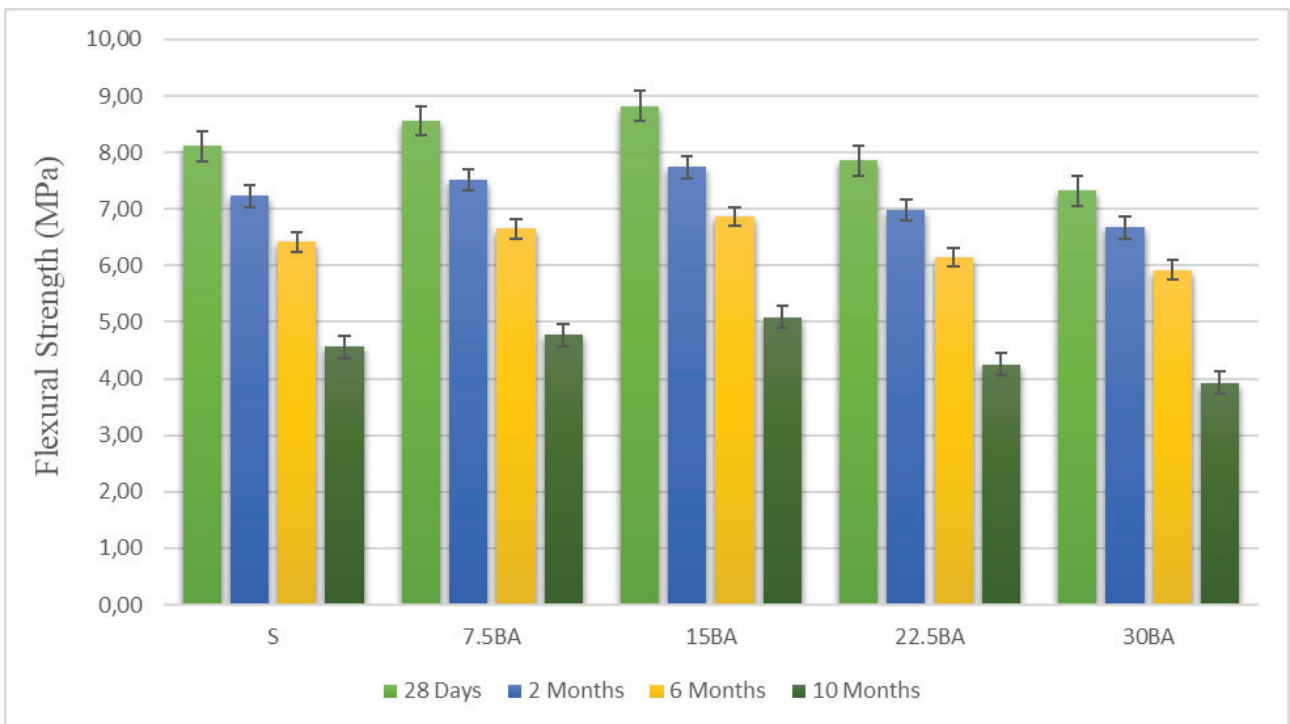


Figure 7. Flexural strength results with sodium chloride exposure.

attacks, in contrast to the compressive strength results [25]. Thus, it was determined that the sensitivity of the flexural strength results was higher. The microcrack propagation in porous structures played an important role in the decrease in flexural strength [26]. In the order of flexural strength results, parallelism was observed with the compressive strengths. This was due to the properties of the solutions.

After 2, 6, and 10 months, residual flexural strengths of 6.52 MPa, 4.98 MPa, and 3.26 MPa were obtained for the 15BA sample under the influence of magnesium sulfate. After 2, 6, and 10 months, residual flexural strengths of 7.32 MPa, 5.73 MPa, and 4.45 MPa were obtained for the 15BA sample under the influence of sodium sulfate. After 2, 6, and 10 months, residual flexural strengths of 7.74 MPa, 6.87 MPa, and 5.09 MPa were obtained for the 15BA sample under the influence of sodium chloride.

### Weight Change Results

Weight values changed under the effect of the solution. These changes can be classified as losses and increases. While the losses occurred mostly with the dissolving of the paste in the solution, the absorption of the geopolymer structure from the solution played a role in the increases [28]. Significant weight gains occurred in all three solution types when the 2 months were completed. The solution absorption to the microstructure was a factor affecting the initial weight gain [29]. That was, sulfate and chloride salts and hydration products played a role in this weight increase by filling the gaps [12]. In addition, the formation of white deposits on the surfaces by reaction products such as gypsum and ettringite was also effective in the weight increase.

Keeping the samples in the oven before the test increased the third rate while increasing the void rate in the pores, which was effective in this weight increase. This increased the effective absorption of the solutions. After 2 months, weight gains were replaced by a decrease in weight gain. In other words, there has been a relative decrease in increasing weight. This was thought to be due to alkalis leaking from the samples into the solution. Partial dissolution and fragmentation of the geopolymer samples, together with this alkali migration event, also contributed to the loss [24]. However, in addition to the weight increase caused by partially filling the pores and cavities and reaching saturation, the dissolutions in the dough structure caused low losses. The relatively small size of the chloride ions increased the penetration, resulting in maximum weight gain. The more aggressiveness of magnesium sulfate resulted in the lowest weight gain [19]. Thus, the order of weight gain was from high to low as sodium chloride, sodium hydroxide, and magnesium sulfate.

The 2-month weight increases were between 4.56% and 5.65%, 6-month weight increases were between 3.86% and 5.02%, and 10-month weight increases were between 3.02% and 3.94% with the magnesium sulfate effect (Figure 8). The 2-month weight increases were between 5.53% and 6.33%, 6-month weight increases were between 4.52% and 5.59%, and 10-month weight increases were between 3.7% and 4.56% with the sodium sulfate effect (Figure 9). The 2-month weight increases were between 6.49% and 7.45%, 6-month weight increases were between 5.42% and 6.34%, and 10-month weight increases were between 4.29% and 5.13% with the sodium chloride effect (Figure 10).

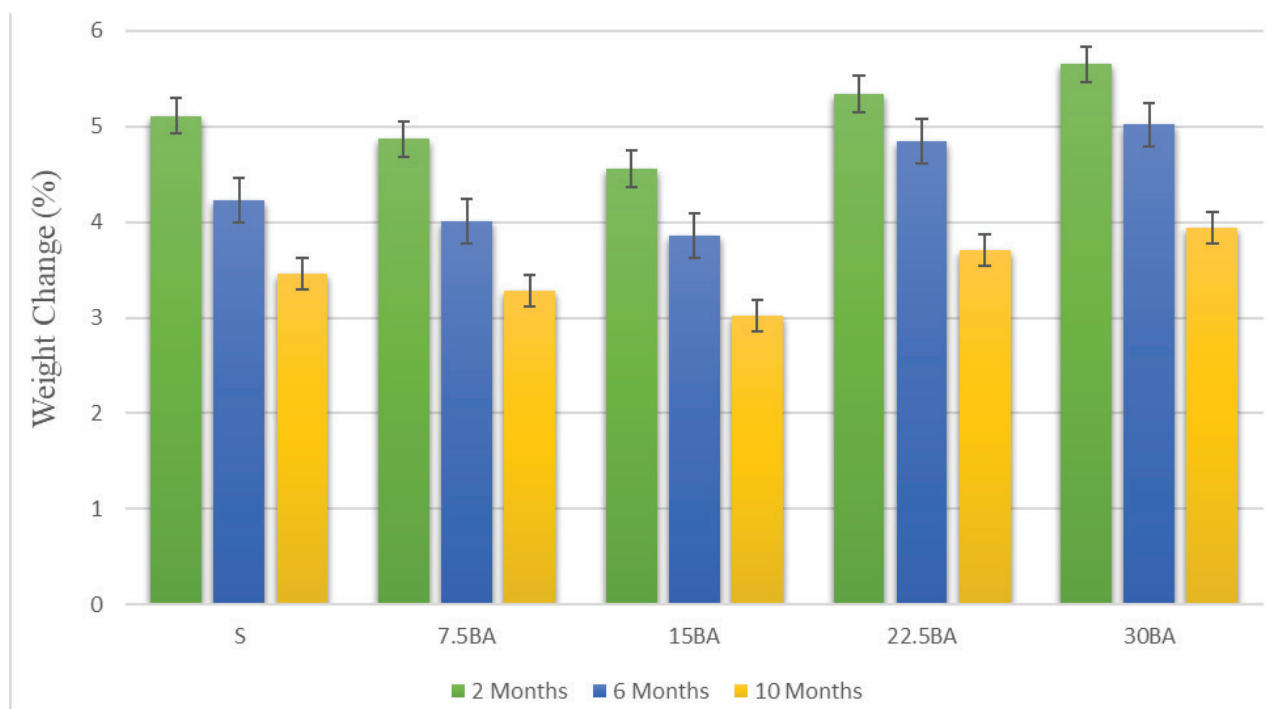


Figure 8. Weight change results from magnesium sulfate exposure.



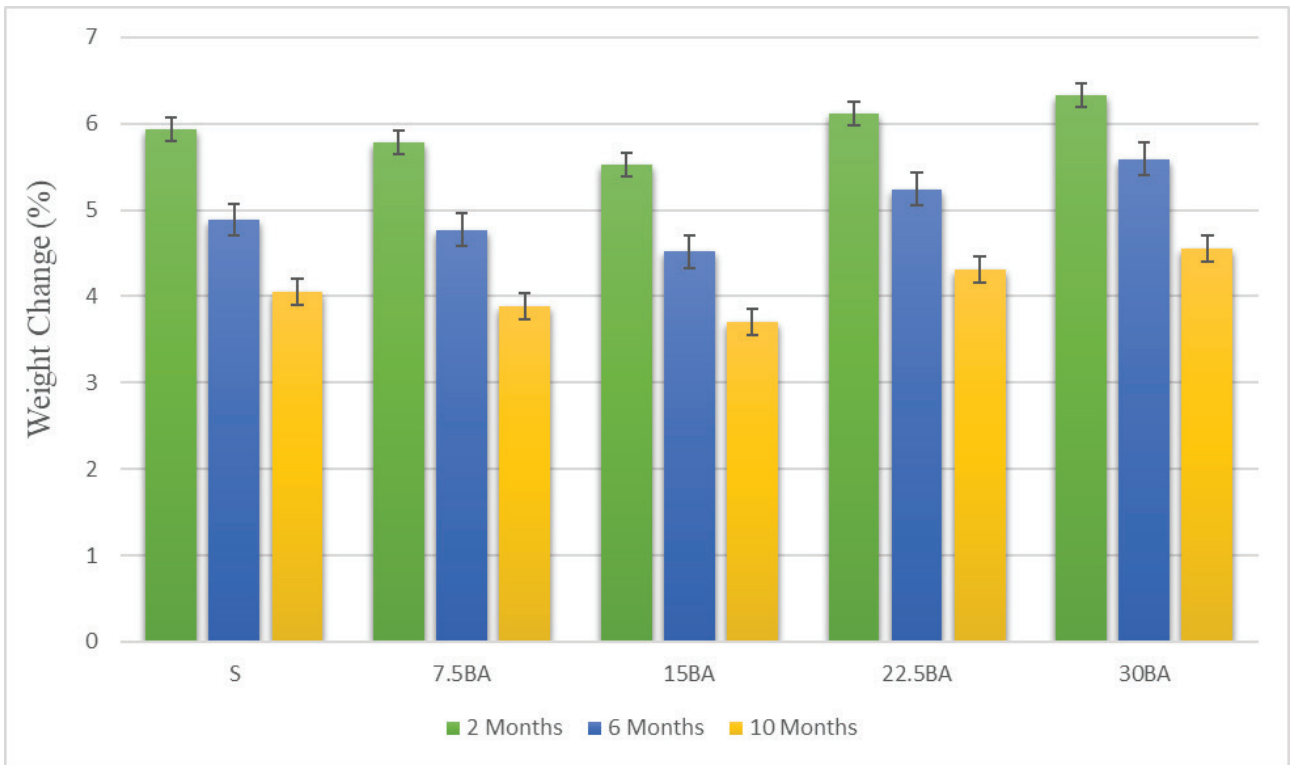


Figure 9. Weight change results from sodium sulfate exposure.

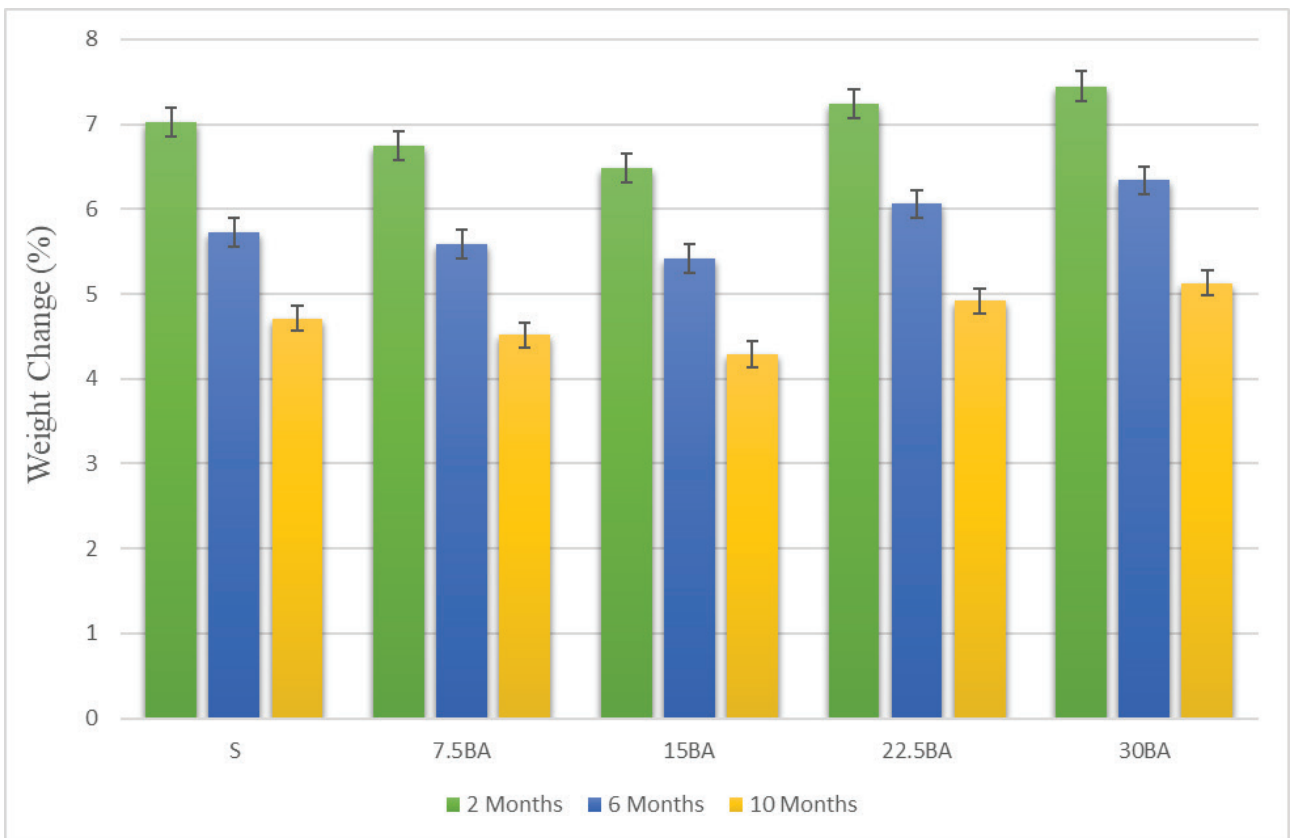


Figure 10. Weight change results from sodium chloride exposure.

### Visual Inspection and Analyzes

To see the effects of the magnesium sulfate test on the microstructure, the SEM analyzes of the S, 7.5BA, and 15BA samples were compared before and after 10 months (Figure 11). While it was seen that the geopolymer gel structure showed a homogeneous behavior before the solution effect, it was observed that the continuity state was stronger in the matrices in the 15BA and 7.5BA samples. This situation has been effective in improving the bond structure with the bottom ash [15, 19-22]. Thus, while a more compact structure was formed, the consistency has also increased. While the effect of magnesium sulfate accelerated the formation of ettringite and gypsum in geopolymer samples, it also increased the expansion stress in the matrix structure [12, 30-31]. Despite this situation, the fact that geopolymer samples had relatively low Ca content compared to cemented samples increased the performance in resistance to sulfate effect. At the same time, the cross and highly stable aluminosilicate structure increased this performance [32-33]. However, it was also known that geopolymerization products showed less sulfate sensitivity compared to the cementitious samples with hydration products [34]. Among these, it has been explained in previous studies that the most important parameter was low Ca content [33].

Although the formation of hydrated calcium silicate gel formed in geopolymerization was observed at a low rate, the aluminosilicate structure with a 3-dimensional frame system, which created a more zeolite-like structure, was seen more intensely [33]. Along with this situation, the fact that the bottom ash had fine particles and filled the voids has also increased the compressive strength of geopolymer

composites. According to the analyzes in detail, it was seen that the slag-based geopolymers showed high performance against chemical solutions. It was seen that the microstructures were generally preserved after magnesium sulfate. While products undergoing expansion and crystals were not observed in the surface microstructures, it was determined that these conditions were observed to a greater extent in the internal microstructure. It was known that the expanding product and crystals were formed when chloride and sulfate ions entered the sample interior from the solution. These conditions increased the porosity and led to the formation of cracking. Thus, some decreases in strength values occurred [35].

Geopolymer samples were visually inspected after magnesium sulfate (Figure 12). According to the examination of the outer surfaces, no significant change was observed, while microcracks were found to be at a low rate. Along with these conditions, exposure to sulfate also produced soft and dust-like deposits. However, despite this situation, corrosion products were not found on the surfaces. Due to these properties, it has been seen that geopolymers were resistant to magnesium sulfate [36].

To see the effects of the magnesium sulfate test on the microstructure, the S, 7.5BA, and 15BA samples were compared before and after the effect with XRD analysis (Figure 13-Figure 14). Quartz crystal peaks were observed in XRD analyzes before the sulfate attack. There was also mullite along with quartz. Quartz peaks between  $20^\circ$  and  $30^\circ$   $2\theta$  indicated that the geopolymerization has taken place at a satisfactory level. Ettringite, anorthite, calcite, and hydroxalcalite were also seen. Magnetite, gismondine, and hematite

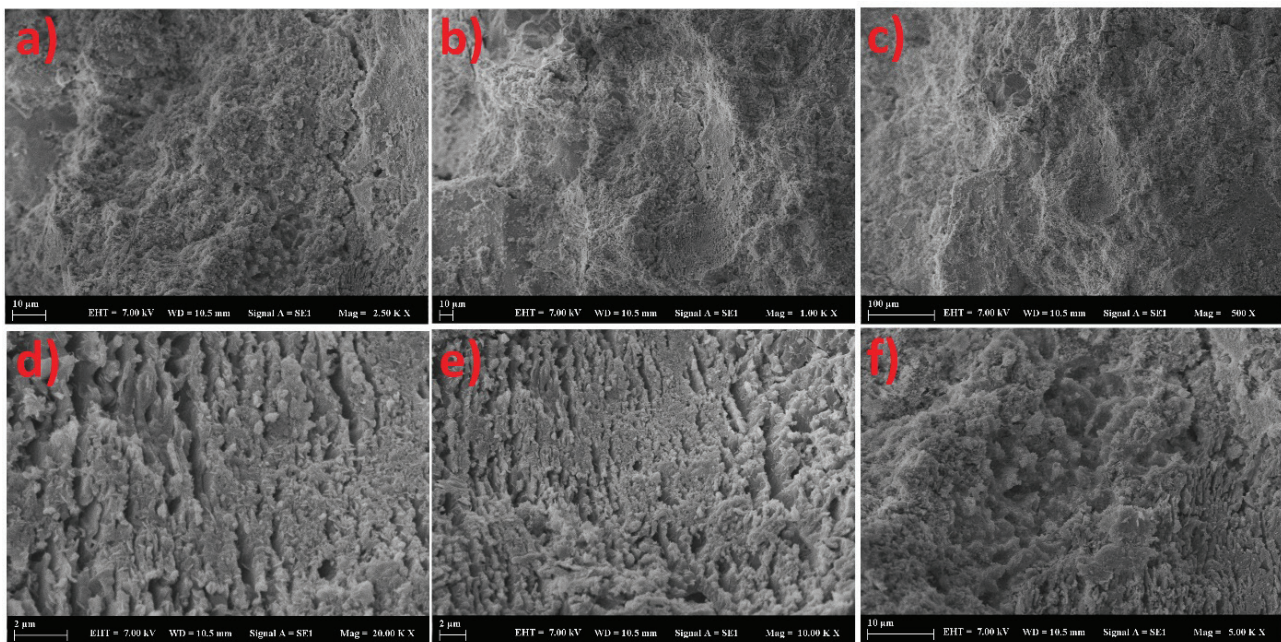


**Figure 11.** SEM images for specimens a)S, b)7.5BA and c)15BA before magnesium sulfate attack and specimens a)S, b)7.5BA and c)15BA after magnesium sulfate attack.



Figure 12. Visual inspection over 10 months after magnesium sulfate effect.

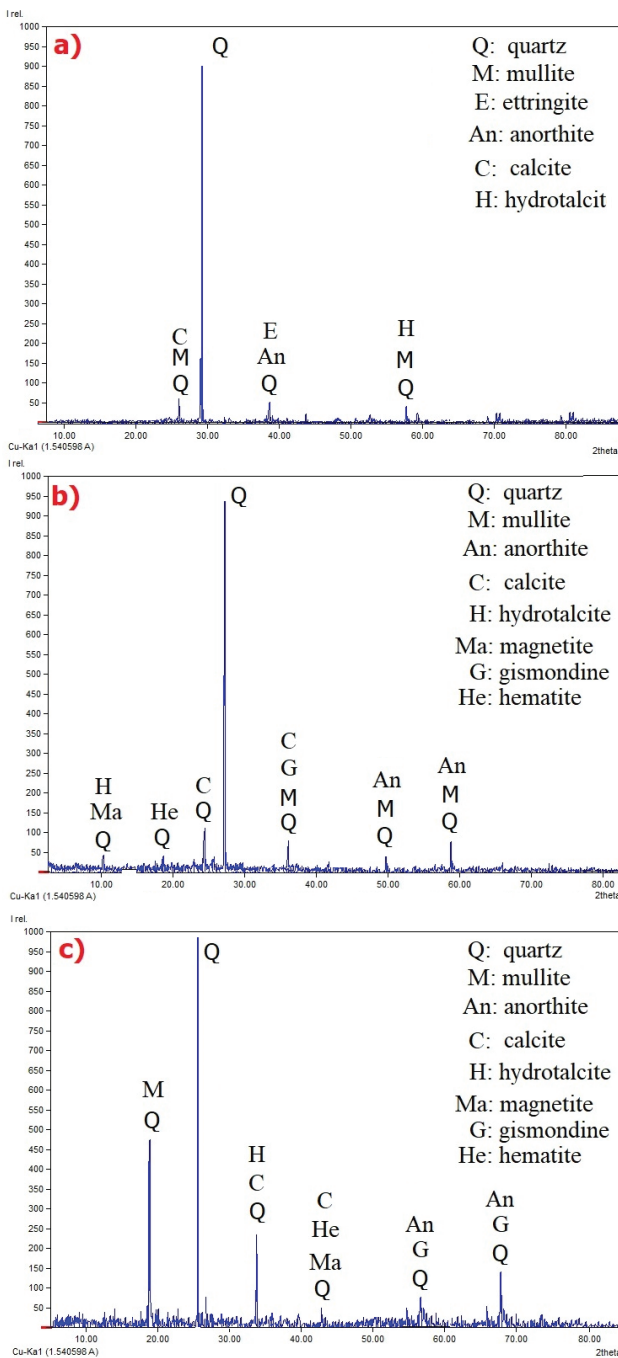


Figure 13. XRD analyses of specimens a) S, b) 7.5BA and c) 15BA before magnesium sulfate attack.

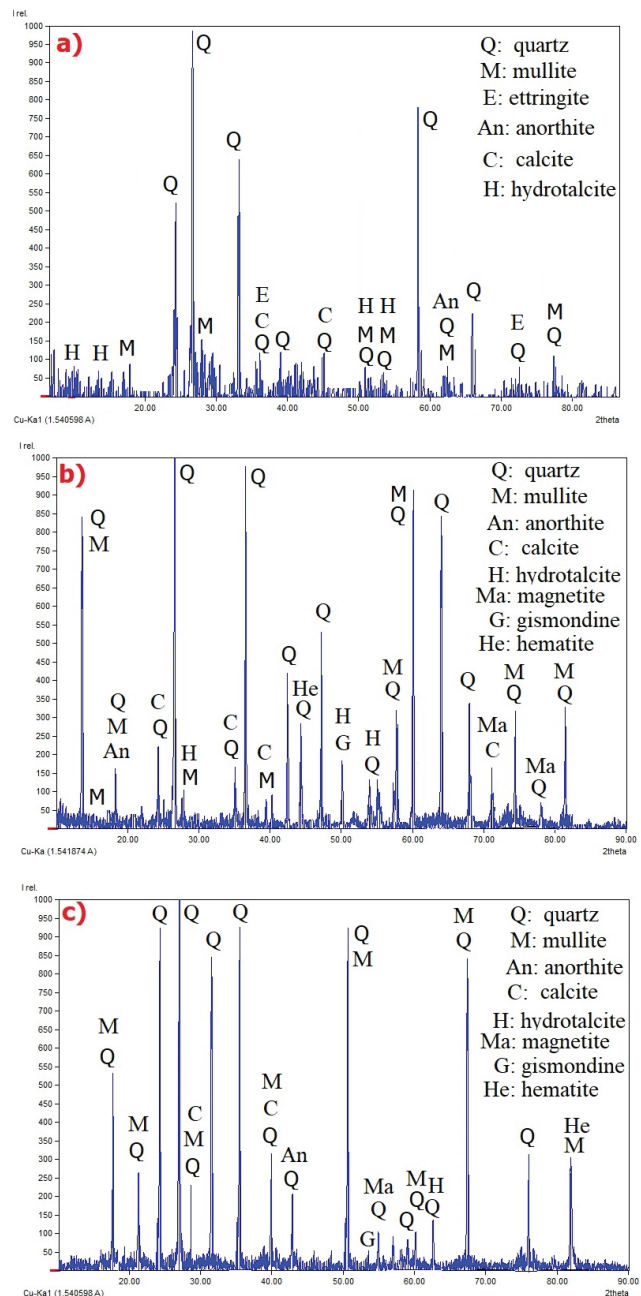


Figure 14. XRD analyses of specimens a) S, b) 7.5BA and c) 15BA after magnesium sulfate attack.

were found in sample 7.5BA and the peak slippage was seen. In the 15BA sample, on the other hand, quartz peaks were formed more intensely with the increase in the amount of silicon oxide [7].

When the XRD analyzes after magnesium sulfate were examined for the same samples, it was seen that the general amorphous phase properties of the geopolymer (between  $18^\circ$  and  $36^\circ 2\theta$ ) changed and the peaks spread between  $18^\circ$  and  $50^\circ 2\theta$ . With the formation of this situation, it was observed that there was an improvement in geopolymerization [36–37]. Consistent with the literature, it has been observed that the binder materials' amorphous phases reacted reactively [36]. In this case, the significant ratio of  $Al_2O_3$  and  $SiO_2$  in the bottom ash material was also effective. It was also effective that sulfate ions penetrated the sample and crystals were produced with the reaction. The interpretations of these results also explained that the geopolymer samples gained strength in 2 months [38]. The gypsum conditions, which were observed in the samples prepared using Portland Cement and caused deterioration under the effect of sulfate, were not observed in the XRD models in geopolymer samples. This was in line with other studies explaining that geopolymers had high resistance to sulfate action [39–42].

## CONCLUSION

For this study, the feasibility of bottom ash reinforcement in the production of slag-based geopolymer composites and the performance of the obtained product against the effect of sulfate and chloride in 10 months were investigated, and the stated results were found:

According to the preliminary test results, a 15% bottom ash substitution was found to be critical in terms of mechanical properties. The utilization of higher bottom ash reduced flowability and workability and resulted in poor performance. For sample 7.5BA, the increased percentages for compressive and flexural strengths according to the control sample were 7.15% and 5.55%, respectively. For sample 15BA, the increase percentages for compressive and flexural strengths according to the control sample were 14.21% and 8.75%, respectively.

While investigating the performance of geopolymer samples against solutions, increases were observed in the compressive strength and weight values over 2 months, while these increases were replaced by a decrease in the following periods. Fluctuations in mechanical properties occurred due to the transitions between the solution and matrix. In addition, being kept in an oven before durability tests facilitated the absorption of the solution. In the next days, the formation of ettringite and gypsum was also effective in the formation of micro-cracks, together with the transition of alkalis to the solution.

The small size of the chloride ions resulted in greater penetration. Magnesium sulfate was known to be more aggressive than sodium sulfate. These conditions ensured

that the weight and compressive strength increases were highest in sodium chloride, followed by sodium sulfate and magnesium sulfate, respectively. In terms of flexural strength, low results were obtained with the magnesium sulfate effect.

When the microstructures were examined after the effect of magnesium sulfate, it was determined according to the SEM analysis that they were preserved. XRD analyzes showed that new crystals were produced and quartz peaks increased with the penetration of sulfate ions into the sample. These conditions indicated that the geopolymerization continued.

Experimental research was carried out within the scope of this study. As a result of the experimental study, a determination was made by using cause-effect relationships among the variables examined. This is a method that is easy and quick to plan, but difficult and time-consuming to execute. Analytical research is a research method by examining and coding the data obtained as a result of experimental studies. By examining the results obtained within the scope of this study with different analytical methods in future studies, it will be possible to have an idea about the situations that may occur under different conditions. For this next study, the experiment can be designed using the Taguchi Method and the model development can be done using the Fuzzy Logic and Artificial Neural Network (ANN) approach.

## DATA AVAILABILITY STATEMENT

The authors confirm that the data that supports the findings of this study are available within the article. Raw data that support the finding of this study are available from the corresponding author, upon reasonable request.

## CONFLICT OF INTEREST

The author declared no potential conflicts of interest with respect to the research, authorship, and/or publication of this article.

## ETHICS

There are no ethical issues with the publication of this manuscript.

## REFERENCES

- [1] Van Deventer JSJ, Provis JL, Duxson P, Brice DG. Chemical research and climate change as drivers in the commercial adoption of alkali activated materials. *Waste Biomass Valorizat* 2010;1:145–155. [CrossRef]
- [2] Bakis A, Isik E, Avsar E. The usability of pumice concrete produced by different kinds of concrete mixing water in construction of rigid pavements. *Fresenius Environ Bull* 2019;28:3649–3657. [CrossRef]

- [3] Bayraktar AC, Avsar E, Toroz I, Alp K, Hanedar A. Stabilization and solidification of electric arc furnace dust originating from steel industry by using low grade MgO. *Arch Environ Prot* 2015;41:62–66. [\[CrossRef\]](#)
- [4] Uslu E, Avşar E, Toröz İ. Otomotiv endüstrisi kimyasal arıtma çamurlarının tuğla üretiminde kullanılabilirliğinin ürün kalitesi yönünden araştırılması. *Sigma J Eng Nat Sci* 2010;3:141–148. [Turkish]
- [5] Chi M, Huang R. Inding mechanism and properties of alkali-activated fly ash/slag mortars. *Constr Build Mater* 2013;40:291–298. [\[CrossRef\]](#)
- [6] Marjanović N, Komljenović M, Baščarević Z, Nikolić V, Petrović R. Physical-mechanical and microstructural properties of alkali-activated fly ash-blast furnace slag blends. *Ceram Int* 2015;41:1421–1435. [\[CrossRef\]](#)
- [7] Zarina Y, Mohd Mustafa ABA, Kamarudin H, Khairul Nizar I, Andrei Victor S, Petrică V, et al. Chemical and physical characterization of boiler ash from palm oil industry waste for geopolymer composite. *Rev Chim* 2013;64:1408–1412.
- [8] Kim SH, Ryu GS, Koh KT, Lee JH. Flowability and strength development characteristics of bottom ash based geopolymer. *Int J Civ Environ Eng* 2012;6:852–857.
- [9] Revathi V, Saravanakumar R, Tharrini J. Effect of molar ratio of  $\text{SiO}_2/\text{Na}_2\text{O}$ ,  $\text{Na}_2\text{SiO}_3/\text{NaOH}$  ratio and curing mode on the compressive strength of ground bottom ash geopolymer mortar. *Int J Earth Sci Eng* 2014;7:1511–1516.
- [10] Guo L, Wu YY, Xu F, Song XT, Ye JY, Duan P, et al. Sulfate resistance of hybrid fiber reinforced metakaolin geopolymer composites. *Compos Part B Eng* 2020;183:1–10. [\[CrossRef\]](#)
- [11] Santhanam M, Cohen MD, Olek J. Mechanism of sulfate attack: a fresh look. *Cem Concr Res* 2003;33:341–346. [\[CrossRef\]](#)
- [12] Bakharev T. Durability of geopolymer materials in sodium and magnesium sulfate solutions. *Cem Concr Res* 2005;35:1233–1246. [\[CrossRef\]](#)
- [13] Fernandez-Jimenez A, García-Lodeiro I, Palomo A. Durability of alkali activated fly ash cementitious materials. *J Mater Sci* 2007;42:3055–3065. [\[CrossRef\]](#)
- [14] Ionescu BA, Lăzărescu AV, Hegyi A. The possibility of using slag for the production of geopolymer materials and its influence on mechanical performances-A review. *Proceedings* 2020;63:30. [\[CrossRef\]](#)
- [15] Tharrini J, Ramasamy V. Properties of foundry sand, ground granulated blast furnace slag and bottom ash based geopolymers under ambient conditions. *Period Polytech Civ Eng* 2016;60:159–168. [\[CrossRef\]](#)
- [16] Qiu J, Zhao Y, Xing J, Sun X. Fly ash/blast furnace slag-based geopolymer as a potential binder for mine backfilling: effect of binder type and activator concentration. *Adv Mater Sci Eng* 2019;2019:2028109. [\[CrossRef\]](#)
- [17] Nis A, Altundal MB. Mechanical strength degradation of slag and fly ash based geopolymer specimens exposed to sulfuric acid attack. *Sigma J Eng Nat Sci* 2019;37:917–926.
- [18] Aygormez, Y. Performance of ambient and freezing-thawing cured metazeolite and slag based geopolymer composites against elevated temperatures. *Rev Constr* 2021;20:145–162. [\[CrossRef\]](#)
- [19] Wongs A, Boonserm K, Waisurasingha C, Sata V, Chindaprasirt P. Use of municipal solid waste incinerator (MSWI) bottom ash in high calcium fly ash geopolymer matrix. *J Clean Prod* 2017;148:49–59. [\[CrossRef\]](#)
- [20] Kumar ML, Revathi V. Metakaolin bottom ash blend geopolymer mortar-A feasibility study. *Constr Build Mater* 2016;114:1–5. [\[CrossRef\]](#)
- [21] Deraman LM, Al Bakri Abdullah MM, Liew YM, Hussin K, Yahya Z. A review on processing and properties of bottom ash based geopolymer materials. *Key Eng Mater* 2015;660:3–8. [\[CrossRef\]](#)
- [22] Hosseini S, Brake NA, Nikookar M, Gunaydin-Sen O, Snyder H. A. (2021). Mechanochemically activated bottom ash-fly ash geopolymer. *Cem Concr Compos* 2021;118:103976. [\[CrossRef\]](#)
- [23] Duan P, Yan C, Zhou W. Influence of partial replacement of fly ash by metakaolin on mechanical properties and microstructure of fly ash geopolymer paste exposed to sulfate attack. *Ceram Int* 2016;42:3504–3517. [\[CrossRef\]](#)
- [24] Elyamany HE, Abd Elmoaty M, Elshaboury AM. Magnesium sulfate resistance of geopolymer mortar. *Constr Build Mater* 2018;184:111–127. [\[CrossRef\]](#)
- [25] Thokchom S, Ghosh P, Ghosh S. Performance of fly ash based geopolymer mortars in sulphate solution. *J Eng Sci Technol Rev* 2010;3:36–40. [\[CrossRef\]](#)
- [26] Zhang HY, Kodur V, Wu B, Cao L, Qi SL. Comparative thermal and mechanical performance of geopolymers derived from metakaolin and fly ash. *J Mater Civ Eng* 2016;28:04015092. [\[CrossRef\]](#)
- [27] Škvára F, Jílek T, Kopecký L. Geopolymer materials based on fly ash. *Ceram Silik* 2005;49:195–204.
- [28] Rashidian-Dezfouli H, Rangaraju PR. A comparative study on the durability of geopolymers produced with ground glass fiber, fly ash, and glass-powder in sodium sulfate solution. *Constr Build Mater* 2017;153:996–1009. [\[CrossRef\]](#)
- [29] Kwasny J, Aiken TA, Soutsos MN, McIntosh JA, Cleland DJ. Sulfate and acid resistance of lithomarge-based geopolymer mortars. *Constr Build Mater* 2018;166:537–553. [\[CrossRef\]](#)
- [30] Müllauer W, Beddoe RE, Heinz D. Sulfate attack expansion mechanisms. *Cem Concr Res* 2013;52:208–215. [\[CrossRef\]](#)
- [31] Maes M, De Belie N. Resistance of concrete and mortar against combined attack of chloride and sodium sulphate. *Cem Concr Compos* 2014;53:59–72. [\[CrossRef\]](#)

- [32] Sata V, Sathonsaowaphak A, Chindapasirt P. Resistance of lignite bottom ash geopolymer mortar to sulfate and sulfuric acid attack. *Cem Concr Compos* 2012;34:700–708. [\[CrossRef\]](#)
- [33] Karakoc MB, Turkmen I, Maras MM, Kantarci F, Demirboga R. Sulfate resistance of ferrochrome slag based geopolymer concrete. *Ceram Int* 2016;42:1254–1260. [\[CrossRef\]](#)
- [34] Chindapasirt P, Kanchanda P, Sathonsaowaphak A, Cao HT. Sulfate resistance of blended cements containing fly ash and rice husk ash. *Constr Build Mater* 2007;21:1356–1361. [\[CrossRef\]](#)
- [35] Ren D, Yan C, Duan P, Zhang Z, Li L, Yan Z. Durability performances of wollastonite, tremolite and basalt fiber-reinforced metakaolin geopolymer composites under sulfate and chloride attack. *Constr Build Mater* 2017;134:56–66. [\[CrossRef\]](#)
- [36] Arslan AA, Uysal M, Yilmaz A, Al-mashhadani MM, Canpolat O, Sahin F, et al. Influence of wetting-drying curing system on the performance of fiber reinforced metakaolin-based geopolymer composites. *Constr Build Mater* 2019;225:909–926. [\[CrossRef\]](#)
- [37] He J, Zhang J, Yu Y, Zhang G. The strength and microstructure of two geopolymers derived from metakaolin and red mud-fly ash admixture: a comparative study. *Constr Build Mater* 2012;30:80–91. [\[CrossRef\]](#)
- [38] Salami BA, Johari MAM, Ahmad ZA, Maslehuudin M. Durability performance of palm oil fuel ash-based engineered alkaline-activated cementitious composite (POFA-EACC) mortar in sulfate environment. *Constr Build Mater* 2017;131:229–244. [\[CrossRef\]](#)
- [39] Ismail I, Bernal SA, Provis JL, Hamdan S, van Deventer JS. Microstructural changes in alkali activated fly ash/slag geopolymers with sulfate exposure. *Mater Struct* 2013;46:361–373. [\[CrossRef\]](#)
- [40] Aygormez Y, Canpolat O, Al-mashhadani MM, Uysal M. Elevated temperature, freezing-thawing and wetting-drying effects on polypropylene fiber reinforced metakaolin based geopolymer composites. *Constr Build Mater* 2020;235:117502. [\[CrossRef\]](#)
- [41] Atahan HN, Arslan KM. Improved durability of cement mortars exposed to external sulfate attack: The role of nano & micro additives. *Sustain Cities Soc* 2016;22:40–48. [\[CrossRef\]](#)
- [42] Yıldırım Ozen M, Dur F, Kunt K, Derun E. Evaluation of gold mine tailings in cement mortar: investigation of effects of chemical admixtures. *Sigma J Eng Nat Sci* 2020;38:2155–2168.